

NASA TECHNICAL
MEMORANDUM



NASA TM X-1223

NASA TM X-1223

FD-503 (FORM 802)

N66-23555 <small>(ACCESSION NUMBER)</small>	1 <small>(THRU)</small>
22 <small>(PAGES)</small>	18 <small>(CODE)</small>
TMX-1223 <small>(NASA OR OR TRIA OR AD NUMBER)</small>	<small>(CATEGORY)</small>

GPO PRICE	\$	
CFSTI PRICE(S)	\$	30
Hard copy (HC)		
Microfiche (MF)		50

ff 653 July 65

EXPERIMENTAL EVALUATION OF SEVERAL
ABLATIVE MATERIALS AS NOZZLE SECTIONS
OF A STORABLE-PROPELLANT ROCKET ENGINE

by Donald A. Peterson and Carl L. Meyer
Lewis Research Center
Cleveland, Ohio

EXPERIMENTAL EVALUATION OF SEVERAL ABLATIVE MATERIALS AS
NOZZLE SECTIONS OF A STORABLE-PROPELLANT ROCKET ENGINE

By Donald A. Peterson and Carl L. Meyer

Lewis Research Center
Cleveland, Ohio

NATIONAL AERONAUTICS AND SPACE ADMINISTRATION

For sale by the Clearinghouse for Federal Scientific and Technical Information
Springfield, Virginia 22151 - Price \$0.30

EXPERIMENTAL EVALUATION OF SEVERAL ABLATIVE MATERIALS AS NOZZLE SECTIONS OF A STORABLE-PROPELLANT ROCKET ENGINE

by Donald A. Peterson and Carl L. Meyer

Lewis Research Center

SUMMARY

23555

Twenty-two ablative-material samples were evaluated as nozzle sections of a storable-propellant (nitrogen tetroxide and a 50-50 percent blend of unsymmetrical dimethylhydrazine with hydrazine) rocket engine to determine general trends among the material variables and to enable comparison of such trends with those observed from similar tests with a hydrogen-oxygen rocket engine reported in NASA TN D-3258. The nominal engine operating conditions for the present investigation included an oxidant-fuel ratio of 2.0, an initial chamber pressure of 100 pounds per square inch absolute, and an initial throat diameter of 1.2 inches.

The ablative-material nozzle samples containing high-purity silica-cloth reinforcement generally had greater erosion resistance than did those containing graphite, carbon, or asbestos reinforcement. Of the high silica-cloth reinforced ablative-material samples, generally those with a phenolic or modified-phenolic resin system had greater erosion resistance than did those samples tested with other resin systems, including phenyl silane, polybenzimidazole, and epoxy novalac. Among comparable material variables, these general trends are in agreement with those reported in NASA TN D-3258.

INTRODUCTION

Ablative materials are being used to provide sacrificial cooling (absorption of heat by mass loss) of rocket-engine thrust chambers in a number of applications. The apparent simplicity and potential reliability of this thrust-chamber cooling technique is attractive, particularly for some applications wherein the more conventional and complex regenerative cooling technique cannot be applied or is marginal. Ablative (sacrificial)

cooling of full thrust chambers presents the problem of minimizing internal-dimensional increases, particularly at the nozzle throat, in order to sustain high engine performance during the required operating life of the chamber and to minimize ablative material wall-thickness requirements. In a rocket engine, the ablative process includes chemical reactions and heat-transfer mechanisms which are not only dependent on the ablative material properties but are also interrelated to the chemical composition and flow properties of the propellant combustion products.

Many of the commercially available ablative materials are rated by the manufacturers on the basis of tests in which high-temperature torches or plasma arcs are used. Such relatively simple tests may provide only approximate indications of the adequacy of a material when subjected to the combustion environment of specific propellant combinations. More sophisticated methods of achieving simulated and controlled propellant combustion environments for tests of ablative materials are being studied. Analytical predictions of the dimensional change of ablative materials subjected to rocket-engine combustion environments is a goal of several computer programs. Such analytical programs are limited in application, at present, by the lack or the accuracy of the required input information relative to material and environmental properties. Confidence in the use of simulated combustion environments or in analytical predictions must be established through correlations with experimental results from tests of materials under rocket-engine combustion environments of interest. Evaluation studies of promising ablative materials in rocket-engine test chambers with specific propellant combinations are required in the development of specific propulsion systems; however, results from such studies are not generally available.

A preliminary investigation (ref. 1) was conducted to evaluate several commercially available ablative materials as nozzle sections of a hydrogen-oxygen rocket engine in order to screen many materials and to identify those materials which appeared most promising. For the investigation of reference 1, the desired nominal engine conditions included an oxidant-fuel ratio of about 6.7 and an initial chamber pressure of 100 pounds per square inch absolute at an initial throat diameter of 1.2 inches. Another investigation, reported herein, was conducted to evaluate further some commercially available ablative materials as nozzle sections of a storable-propellant (nitrogen tetroxide and a 50-50 percent blend of unsymmetrical dimethylhydrazine with hydrazine) engine in order to screen again materials and to identify those which appeared most promising. These investigations, further, provided experimental results which can be used as a basis of comparison for results from analytical predictions or simulated combustion environments. For the investigation reported herein, the desired nominal engine conditions included an oxidant-fuel ratio of 2.0 and an initial chamber pressure of 100 pounds per square inch at an initial throat diameter of 1.2 inches (nominal thrust of 150 lb). Results from tests of 22 ablative-material samples are presented and discussed herein primarily in terms of

nozzle throat dimension increase as a function of accumulated run time (from successive runs) in order to determine general trends among the material variables. Such trends are also discussed relative to those reported in reference 1. No attempt was made to select the best material.

ABLATIVE-MATERIAL SAMPLES

The ablative-material samples evaluated in the present investigation are listed in table I. The samples have been numbered in the order presented in the table, and this number is used herein to identify the samples. An NASA code number (assigned to each sample when received), the sample supplier, and material code number for each sample are given also in table I for cross reference. In addition, the table lists available material information as to the reinforcement, fiber orientation, resin, resin modification or additives, and molding conditions. Twelve of the materials included high-purity silica-cloth reinforcement and phenolic resin, without and with modifications or additives. Five of the materials included phenolic resin with reinforcements other than high silica cloth, including asbestos cloth and paper, carbon cloth, and graphite cloth. The fiber orientation is given relative to the nozzle centerline. Sixteen of the samples had fiber orientation perpendicular to the nozzle centerline. For three samples (11, 15, and 16), the fibers were directed downstream at 60° to the nozzle centerline. The 1/2 by 1/2 designation indicates nozzles (9, 10, and 21) made from molded blocks of material reinforced with 1/2-inch squares of woven fiber.

APPARATUS

Facility

The experimental runs were conducted in a small rocket-engine test facility shown in figure 1. A schematic diagram of the installation is given in figure 2. The fuel and oxidant tanks were pressurized with gaseous nitrogen; tank pressures were controlled by pressure regulators at pressure levels preselected for each firing.

Basic Engine

The basic engine configuration is shown disassembled and assembled in figure 3. The configuration used for most of the tests provided nominally a length L of 13.5 inches,

a characteristic length L^* of 65 inches, and a contraction ratio of 6 (throat diameter, 1.2 in.).

The injector (fig. 4) included 10 balanced triplet elements in a circular pattern; each element consisted of two oxidant streams impinging on a single central fuel stream. Three injectors of the same configuration were used in the program; one of these injectors was used for most of the tests.

The combustion chamber (fig. 3(b)) consisted of water-cooled sections including a short conical section at the injector end, either two or three cylindrical spool sections of 2.875-inch inside diameter and 3-inch length, and generally another short conical adapter section at the downstream end to reduce the inside diameter to 2.31 inches at the entrance to the nozzle section. The combustion chamber included three of the cylindrical spool sections for most of the tests.

A heat-sink metal nozzle (fig. 5) with a contoured throat was used to permit definition of throat area in evaluating and checking the combustion performance from short-duration firings.

Ablative-Material Nozzle Sections

The ablative-material samples, as received, were generally 3.5- to 4.0-inch-diameter cylinders, nominally 4 inches in length, or nominally 4-inch cubes; it was thought that differences in external geometry would not affect the erosion characteristics of the samples. The samples were machined to form nozzle sections with the fiber orientations indicated in table I. The internal entrance diameter of the ablative-material nozzle section was 2.35 inches for all but two of the samples; samples 5 and 8 had inlet entrance diameters of 2.94 inches and were used without the downstream conical adapter section (fig. 3(b)). The inside diameter of all but five (6, 10, 14, 15, and 22) nozzle samples converged conically to a 1.2-inch-diameter tubular throat, which was 1 inch long (fig. 6(a)). Samples 6, 10, and 22 included a contoured throat as illustrated in figure 6(b). The materials of interest in samples 13, 14, and 15 were used as "throat inserts" installed in a backup ablative material; these configurations are illustrated in figure 6(c) for sample 13 and figure 6(d) for samples 14 and 15.

Two methods were used to attach the ablative-material nozzle sections to the combustion chamber. In most instances, the internally machined ablative-material nozzle sections were simply held to and sealed against the combustion chamber only by pressure applied with pneumatic clamps. In other cases, the ablative-material nozzle sections were inserted into a metal sleeve with a fixed metal retainer ring at the downstream end, and a metal retainer ring was hand screwed into place at the upstream end of the nozzle; the resultant assembly was held to forward sections of the engine by pneumatic clamps.

This latter method is illustrated in figure 3. Both attachment methods were also used in the investigation of reference 1.

Instrumentation

The combustion-chamber pressure was taken from a tap on the injector face and measured by strain-gage-type pressure transducers. The flow rates of each propellant were measured by both a venturi and a turbine-type flowmeter. Thrust was not measured. Pressure and flow-rate outputs were continuously recorded on a multichannel, variable-speed oscillograph. Backup data were monitored on self-balancing potentiometer strip charts.

PROCEDURE

The instrumentation was calibrated and the engine was pressure checked prior to each run. The propellant tank pressures were set at values selected to provide the desired nominal chamber pressure and oxidant-fuel ratio. For test runs with ablative-material nozzle sections, the initial conditions for each run were planned to include nominally a chamber pressure of 100 pounds per square inch absolute and an oxidant-fuel ratio of 2; owing to lack of an available closed-loop controller, considerable deviations in initial conditions of pressure and oxidant-fuel ratio occurred because of inaccuracies in setting propellant tank pressures. Some variation in oxidant-fuel ratio occurred as chamber pressure decayed during a run. Termination of each run was planned when the chamber pressure had decayed to 90 pounds per square inch absolute or the propellant supply was exhausted, whichever occurred first; considerable deviations occurred in final chamber pressure, primarily because of inaccuracies in setting the low chamber pressure cutoff. A sequence timer automatically activated appropriate valves, data acquisition equipment, and duration of propellant line purges for each run.

The throat diameter of all ablative-material nozzles was measured before and after each run. An optical comparator with a magnification of 10 was used to obtain an outline of the nozzle throat; an effective diameter was calculated from the planimetered area. Generally, each ablative-material sample was subjected to successive runs until the throat area had increased by 50 percent or more. Each sample was subsequently sectioned for inspection and photographing.

Combustion performance was evaluated and checked periodically. The performance runs were accomplished by substituting a metal heat-sink nozzle for the ablative-material nozzle sections and conducting short-duration firings, generally over a range of oxidant-

fuel ratio. Combustion performance level was based on characteristic velocity efficiency. The experimental characteristic velocity was calculated through use of the measured injector-end chamber pressure, propellant flow rate, and nozzle throat area; corrections were not made for momentum pressure loss or nozzle thermal expansion.

RESULTS AND DISCUSSION

Combustion Performance

As pointed out previously, three injectors of the same configuration were used in the program, though one of these was used for most of the runs. In addition, two combustion chamber lengths were used, with the longer chamber used for most of the runs. The nominal characteristic lengths associated with these chambers were 50 and 65 inches.

The majority of the performance checks with the metal nozzle were made with the injector and long chamber used in most of the ablative-material nozzle tests. From consideration of the characteristic-velocity efficiencies from these performance checks, together with available efficiencies from performance checks with the other chamber length or injectors, it was considered impossible to discern definitely combustion performance differences attributable to injector, combustion-chamber length, or oxidant-fuel ratios from 1.5 to 2.3. The characteristic-velocity efficiencies based on chamber pressure measurement indicated a mean level of 0.957 ± 0.032 , with 70 percent of all data within this range. It is believed, however, that the characteristic-velocity efficiency did not vary significantly during the program and that the aforementioned data spread is representative of inaccuracies associated with calculating characteristic velocity based on chamber pressure.

Throat Erosion of Ablative-Material Nozzle Sections

Table II presents a summary for each of the ablative-material nozzle sections of the run durations, run conditions in terms of chamber pressure and oxidant-fuel ratio, and a history of the throat dimension before and after each run. The increase in throat dimension as a function of accumulated run time from successive runs was selected as the basis of comparison for determining general trends among the material variables. It was the intention that all ablative-material nozzle sections be subjected to essentially identical test conditions. It was pointed out previously and is apparent from the table, however, that appreciable deviations occurred in initial chamber pressure, amount of chamber-pressure decay, and oxidant-fuel ratio among the various runs. Because of these deviations, exact quantitative comparisons between ablative-material samples are not war-

ranted. General qualitative trends among major material variables, however, should be valid.

The increase in throat dimension as a function of accumulated run time (from successive runs) is shown graphically, based on the data of table II, in figures 7 to 9. The results for materials including high silica-cloth reinforcement and phenolic resin, without and with modifications, are shown in figure 7. Figure 8 includes the results for materials with high silica-cloth reinforcement but resins other than phenolic, including epoxy novalac, phenyl silane, and polybenzimidazole. The results for materials with phenolic resin and reinforcements other than high silica cloth, including asbestos cloth and paper, carbon cloth, and graphite cloth, are presented in figure 9. Generally, all available data are included regardless of the deviations in run conditions and ablative-material nozzle-section configurations. Smooth curves were faired to represent the trends of the data. Lines of constant erosion rate have been superimposed on the figures as a comparative background.

The two samples with high silica-cloth reinforcement and phenolic resin without modification had generally comparable erosion resistance (fig. 7(a)). The erosion rate increased with accumulated run time; this was generally characteristic for all materials, as can be observed in the remaining figures.

Of the three samples with high silica-cloth reinforcement and phenolic resin modified with silica powder (fig. 7(b)), samples 3 and 4 had comparable erosion resistance and were somewhat less erosion resistant than the materials with an unmodified phenolic resin. The results indicate that the third sample (5) had significantly greater erosion resistance than the other two comparable samples or those with an unmodified resin. The reasons for the greater erosion resistance of sample 5 are not apparent but may include (a) an enlarged entrance diameter (2.94 against 2.35) and (b) fabrication or basic material variables.

Of the samples with high silica-cloth reinforcement and phenolic resin modified with a polyamide resin (fig. 7(c)), two samples (7 and 8) had comparable erosion resistance and were somewhat more erosion resistant than the materials with an unmodified resin. The other two (6 and 9) had lower erosion resistance, possibly because of the initially contoured throat of sample 6 (fig. 6(b)) and the molded 1/2-inch squares of reinforcement of sample 9.

The three samples for which results are presented in figure 7(d) include different modifications. Sample 10 included an inorganic modification and was less erosion resistant than the other two or the materials with unmodified phenolic resin, probably partly because of both an initially contoured throat as well as the molded 1/2-inch squares of reinforcement. Sample 11 also included an inorganic modification and was somewhat more erosion resistant in its early life but less erosion resistant in the later firings than the materials with unmodified phenolic resin. Sample 12 was more erosion resistant than

the other two. Its erosion resistance was significantly greater than that of the materials with unmodified resin in its early life, possibly because of protection provided by the chromium salts added to the reinforcement; subsequent increased erosion rates, however, lead to its dimensional change being comparable with the materials with unmodified resins after an accumulated firing time of 108 seconds.

The results in figure 8, for samples with high silica-cloth reinforcement and phenyl silane, polybenzimidazole, and epoxy novalac resins do not indicate any major differences between these three resin systems. All these samples were less erosion resistant than the samples with unmodified phenolic resin.

The samples for which results are presented in figure 9 include phenolic resins with asbestos, carbon, and graphite reinforcement. All these samples were less erosion resistant than high silica-cloth reinforcement. Of these samples, those with graphite cloth reinforcement had the greatest and those with asbestos reinforcement the least erosion resistance. Of the two samples reinforced with graphite cloth, the one (21) with molded 1/2-inch squares of reinforcement had the least erosion resistance. A primary failure mode of the samples containing carbon and graphite would seem to be oxidation; graphite cloth, with higher oxidation resistance than carbon cloth, had the greater erosion resistance of the two.

The results of tests of the 22 ablative samples are summarized in figure 10 on the basis of the faired curves (figs. 7 to 9) of throat radius increase as a function of accumulated run time from successive runs. The ablative-material nozzle samples containing high-purity silica-cloth reinforcement generally had greater erosion resistance than did those containing graphite, carbon, or asbestos reinforcement. Of the high silica-cloth reinforced ablative-material nozzle samples, generally those with a phenolic or modified-phenolic resin system had greater erosion resistance than did those samples tested with other resin systems, including phenyl silane, polybenzimidazole, and epoxy novalac. Materials for which the reinforcement fibers had specific orientations relative to the nozzle centerline generally had greater erosion resistance than did three comparable samples reinforced with 1/2-inch squares of woven fiber.

No attempt was made to specify molding conditions for the material samples tested. The results of figure 10 were considered with respect to the molding variables listed in table I; however, no consistent trends were apparent with respect to molding pressure, temperature, or time.

The results of the present investigation confirm those of reference 1 relative to general trends among comparable material variables; the results of reference 1 were obtained from tests with a hydrogen-oxygen rocket engine as compared with use of a storable-propellant engine in the present investigation. Reference 1 states that (a) of the reinforcing materials, only silica cloth exhibited relatively good erosion resistance and (b) of the materials tested, those using silica-cloth reinforcement with a polyamide-modified phe-

nolic resin or a silica-powder-modified phenolic resin exhibited the highest erosion resistance.

The apparent erosion resistance of comparable ablative-material nozzle samples was appreciably less in the present investigation than in the investigation of reference 1. In the present investigation, the accumulated run time for a given throat radius change (113 mils) was from 6 to 50 percent of that in the investigation of reference 1 with comparable materials. The entire reasons for this behavior are not known. The theoretical maximum combustion temperatures, at the nominal test values of oxidant-fuel ratio and chamber pressure for the two investigations, were approximately equal. Higher actual combustion temperature in the present investigation, however, because of the higher characteristic-velocity efficiency as compared with that for the investigation of reference 1 (0.957 against approx. 0.93), is certainly a major factor. It is also possible that other characteristics attributable to the injector patterns contributed to the differences in apparent erosion resistance of comparable ablative materials. Differences in chemical species of the combustion products for the two investigations may also be a factor.

Although the relation of erosion rate to char formation was not a primary objective of this report, figure 11 shows typical char formation for samples 1, 10, and 19. All three, as shown, have eroded to a throat diameter of approximately 1.50 inches, sample 1 in 99.6 seconds, sample 10 in 54.5 seconds, and sample 19 in only 24.8 seconds. The desirability of producing a thick, tenacious char is obvious on the basis of erosion; however, such factors as added weight due to increased wall thickness must also be considered if excessive charring at a constant erosion rate is experienced.

SUMMARY OF RESULTS

An investigation was conducted to evaluate 22 commercially obtained ablative material samples as nozzle sections of a storable-propellant (nitrogen tetroxide and a 50-50 percent blend of unsymmetrical dimethylhydrazine with hydrazine) rocket engine in order to determine general trends among the material variables and to enable comparison of such trends with those reported in NASA TN D-3258 from similar tests with a hydrogen-oxygen engine. Results from the investigation reported herein are summarized as follows:

1. The ablative-material nozzle samples containing high silica-cloth reinforcement generally had greater erosion resistance than did those containing graphite, carbon, or asbestos reinforcement.

2. Of the high silica-cloth reinforced ablative-material samples, generally those with a phenolic or modified-phenolic resin system had greater erosion resistance than did those samples tested with other resin systems, including phenyl silane, polybenzi-

midazole, and epoxy novalac.

3. Three ablative-material samples with molded 1/2-inch squares of reinforcement had less erosion resistance than comparable samples for which the fibers had specific orientations relative to the nozzle centerline.

4. The results of the present investigation are in agreement with those of NASA TN D-3258 relative to general trends among comparable material variables. The apparent erosion resistance of comparable ablative-material samples, however, was appreciably less in the present investigation than in the investigation reported in NASA TN D-3258; this difference is attributed to higher characteristic-velocity combustion performance in the present investigation and possibly to other characteristics of the propellant injector patterns.

Lewis Research Center,
National Aeronautics and Space Administration,
Cleveland, Ohio, December 7, 1965.

REFERENCE

1. Salmi, Reino J.; Wong, Alfred,; and Rollbuhler, R. James: Experimental Evaluation of Various Nonmetallic Ablative Materials as Nozzle Sections of Hydrogen-Oxygen Rocket Engine. NASA TN D-3258, 1966.

TABLE I. - DESCRIPTION OF ABLATIVE-MATERIAL SAMPLES

Sample	NASA code number	Sample supplier	Material code number	Reinforcement			Resin		Resin modification or additive		Molding conditions		
				Type	Amount, weight percent	Fiber orientation	Type	Amount, weight percent	Type	Amount, weight percent	Temperature, °F	Pressure, lb/sq in.	Time, hr
1	47-3	Fiberite	MX2641	Silica cloth	70	90°	Phenolic	30	None	300	1000	8	
2	65-2	Cin. Test. Labs.	-----		72			28	None	280	200	6	
3	66-2	Cordo	R84-ACX		75			--	Silica	325	1000	2	
4	67-2	Haveg	MX2600		61			31	Silica powder	310	5500	3.5	
5	30-3	Fiberite	MXS75		61			31	Silica powder	310	1000	6	
6	33-2	Haveg	PLIV-2		80			20	Polyamide	310	3500	3	
7	68-2	Haveg	MX2646		80			20		310	5500	3.5	
8	28-3	Fiberite	MXS19		68			32		305	1000	4	
9	43-2	Fiberite	MX2646		80	1/2 by 1/2		20		310	4000	4	
10	32-4	Haveg	PLIV-1		64	1/2 by 1/2		30	Ceramic frit	310	3500	3	
11	54	U. S. Polymeric	FM5067		--	60°		--	Ceramic frit	310	1750	1.5	
12	70	HITCO	IRISH		--	90°		--		---	---	---	
13	47-29	AVCO	-----		67	90°	Epoxy novalac	33	None	---	---	---	
14	47-E	AVCO	2001		70	90°	Epoxy novalac	30	None	325	200	---	
15	47-D	AVCO	2001		70	60°	Epoxy novalac	30	None	325	200	---	
16	56	U. S. Polymeric	XR2015		--	60°	Phenyl silane	--	Buna N	325	1000	1.5	
17	63	NARMCO	1850		--	90°	Polybenzimidazole	--	None	700	200	3	
18	41-2	Raybestos Man.	41RPD	Asbestos cloth	73		Phenolic	27		300	500	0.5	
19	36-2	Johns Manville	ARP40	Asbestos paper	60			40		---	---	---	
20	71	HITCO	-----	Carbon cloth	--			--		---	---	---	
21	31	Haveg	FM5014	Graphite cloth	--	1/2 by 1/2		--		---	---	---	
22	69	Fiberite	MX4500	Graphite cloth	75	90°		--		310	1000	3	

TABLE II. - SUMMARY OF TEST RESULTS

Sample	NASA code number	Nozzle configuration			Firing time, sec	Firing conditions			Throat diameter, in.		Accumulated firing time, sec	Accumulated change in throat radius, in.	Change in throat radius with time, $\Delta r/\Delta t$, mils/sec	Accumulated change in throat radius with time, $\Delta r/\Delta t$, mils/sec	Figure (Δr plotted against Δt)			
		Inlet diameter, in.	Throat type	Figure		Chamber pressure, lb/sq in. abs	Average oxidant-fuel ratio	Initial	Final	Initial						Final		
																	Initial	Final
1	47-3	2.35	Tubular	6(a)	26.6	100.5	89.0	1.860	1.200	1.250	26.6	0.025	0.94	0.94	7(a)			
					34.1	97.0	94.0	2.431	1.250	1.352	60.7	.076	1.50	1.25	7(a)			
					38.9	99.0	89.0	2.209	1.352	1.500	99.6	.150	1.90	1.51	7(a)			
2	65-2	2.35	Tubular	6(a)	50.7	103.5	89.0	2.175	1.200	1.320	50.7	0.060	1.18	1.18	7(a)			
					19.5	98.5	95.0	2.265	1.320	1.372	70.2	.086	1.33	1.23	7(a)			
					15.7	93.5	91.0	1.839	1.372	1.403	85.9	.102	.99	1.19	7(a)			
					27.6	104.0	90.5	1.624	1.403	1.569	113.5	.185	3.01	1.63	7(a)			
3	66-2	2.35	Tubular	6(a)	36.5	102.0	87.0	1.935	1.200	1.311	36.5	0.056	1.53	1.53	7(b)			
					34.2	95.5	86.5	2.210	1.311	1.442	70.7	.121	1.91	1.71	7(b)			
					24.0	111.5	109.5	1.875	1.442	1.552	94.7	.176	2.29	1.86	7(b)			
4	67-2	2.35	Tubular	6(a)	53.2	107.0	88.5	1.690	1.200	1.360	53.2	0.080	1.50	1.50	7(b)			
					21.3	92.0	86.5	2.120	1.360	1.441	74.5	.121	1.90	1.62	7(b)			
					29.5	98.5	85.5	1.995	1.441	1.586	104.0	.193	2.46	1.86	7(b)			
5	30-3	2.94	Tubular	6(a)	36.9	101.5	99.0	2.227	1.200	1.204	36.9	0.002	0.05	0.05	7(b)			
					55.5	103.5	93.0	2.282	1.204	1.337	92.4	.069	1.20	.75	7(b)			
					23.6	96.5	92.0	2.040	1.337	1.420	116.0	.110	1.76	.95	7(b)			
					26.4	100.0	91.0	1.812	1.420	1.530	142.4	.165	2.08	1.16	7(b)			
6	33-2	2.35	Contour	6(b)	35.3	106.5	91.0	2.027	1.200	1.290	35.3	0.045	1.27	1.27	7(c)			
					19.2	98.5	91.0	1.876	1.290	1.379	54.5	.090	2.32	1.65	7(c)			
					18.0	97.5	91.0	1.599	1.379	1.470	72.5	.135	2.53	1.86	7(c)			
7	68-2	2.35	Tubular	6(a)	27.0	95.5	90.5	2.150	1.200	1.200	27.0	0.000	0.00	0.00	7(c)			
					25.2	97.5	93.5	1.736	1.200	1.295	52.2	.048	1.88	.91	7(c)			
					12.2	94.0	89.0	1.905	1.295	1.348	64.4	.074	2.17	1.15	7(c)			
					17.6	93.0	89.0	2.464	1.348	1.424	82.0	.112	2.16	1.37	7(c)			
					22.3	97.5	92.0	2.051	1.424	1.495	104.3	.148	1.59	1.42	7(c)			
8	28-3	2.94	Tubular	6(a)	54.1	101.5	89.5	2.167	1.200	1.288	54.1	0.044	0.81	0.81	7(c)			
					24.9	96.5	90.5	1.744	1.288	1.367	79.0	.084	1.59	1.06	7(c)			
					24.7	105.0	91.0	1.732	1.367	1.525	103.7	.163	3.20	1.57	7(c)			
9	43-2	2.35	Tubular	6(a)	47.3	109.0	86.5	1.612	1.200	1.333	47.3	0.067	1.42	1.42	7(c)			
					38.1	106.5	87.0	2.106	1.333	1.616	85.4	.208	3.71	2.44	7(c)			
10	32-4	2.35	Contour	6(b)	27.7	100.5	92.5	1.894	1.200	1.298	27.7	0.049	1.77	1.77	7(d)			
					12.0	98.5	92.5	1.758	1.298	1.362	39.7	.081	2.67	2.04	7(d)			
					14.8	101.5	90.5	1.815	1.362	1.480	54.5	.140	3.99	2.57	7(d)			
11	54	2.35	Tubular	6(a)	44.3	100.0	90.0	1.686	1.200	1.252	44.3	0.026	0.59	0.59	7(d)			
					22.6	102.0	91.5	1.987	1.252	1.392	66.9	.096	3.10	1.43	7(d)			
					11.8	97.0	93.0	2.015	1.392	1.452	78.7	.126	2.54	1.60	7(d)			
					12.0	96.0	91.0	1.847	1.452	1.545	90.7	.173	3.88	1.91	7(d)			

TABLE II. - Concluded. SUMMARY OF TEST RESULTS

Sample	NASA code number	Nozzle configuration			Firing time, sec	Firing conditions			Throat diameter, in.		Accumulated firing time, sec	Accumulated change in throat radius, in.	Change in throat radius with time, $\Delta r/\Delta t$, mils/sec	Accumulated change in throat radius with time, $\Delta r/\Delta t$ mils/sec	Figure (Δr plotted against Δt)	
		Inlet diameter, in.	Throat type	Figure		Chamber pressure, lb/sq in. abs		Average oxidant-fuel ratio	Initial	Final						
						Initial	Final									
12	70	2.35	Tubular	6(a)	46.6	93.0	90.0	1.525	1.200	1.220	46.6	0.010	0.21	0.21	7(d)	
					^a 13.7	-----	-----	-----	-----	-----	60.3	-----	-----	-----	-----	7(d)
					32.8	103.5	89.0	1.760	-----	1.398	93.1	.099	1.91	1.06	7(d)	
					14.6	98.5	94.0	1.977	1.398	1.521	107.7	.161	4.21	1.49	7(d)	
13	47-29	2.35	Tubular	6(c)	50.3	103.7	88.5	2.153	1.200	1.400	50.3	0.100	1.99	1.99	8	
					25.5	104.1	89.5	2.251	1.400	1.570	75.8	.185	3.33	2.44	8	
14	47-E	2.35	Contour	6(d)	37.0	98.0	90.5	1.881	1.200	1.282	37.0	0.041	1.11	1.11	8	
					40.0	102.5	89.0	1.952	1.282	1.560	77.0	.180	3.48	2.34	8	
15	47-D	2.35	Contour	6(d)	32.5	94.0	86.5	1.629	1.200	-----	32.5	-----	-----	-----	8	
					18.0	97.5	88.0	1.744	-----	1.370	50.5	0.085	-----	1.68	8	
					20.7	100.5	90.5	1.772	1.370	1.474	71.2	.137	2.51	1.92	8	
16	56	2.35	Tubular	6(a)	31.9	103.0	89.5	1.806	1.200	1.290	31.9	0.045	1.41	1.41	8	
					19.5	100.5	89.0	1.859	1.290	1.456	51.4	.128	4.26	2.49	8	
					15.5	100.0	91.0	1.984	1.456	1.556	66.9	.178	3.23	2.66	8	
17	63	2.35	Tubular	6(a)	30.0	100.0	88.0	1.816	1.200	1.305	30.0	0.053	1.77	1.77	8	
					12.8	93.5	89.0	1.952	1.305	1.366	42.8	.083	2.38	1.94	8	
					10.8	91.0	88.0	2.003	1.366	1.419	53.6	.110	2.45	2.05	8	
					24.4	94.5	89.0	2.112	1.419	1.486	78.0	.143	1.37	1.83	8	
18	41-2	2.35	Tubular	6(a)	11.0	104.5	98.5	2.050	1.200	1.353	11.0	0.077	7.00	7.00	9	
					7.2	92.0	89.5	2.039	1.353	1.506	18.2	.153	10.6	8.41	9	
19	36-2	2.35	Tubular	6(a)	15.2	101.0	88.5	2.009	1.200	1.352	15.2	0.076	5.00	5.00	9	
					9.6	105.5	89.5	1.851	1.352	1.513	24.8	.157	8.39	6.33	9	
20	71	2.35	Tubular	6(a)	15.7	96.0	93.0	1.539	1.200	1.257	15.7	0.029	1.85	1.85	9	
					18.1	101.0	89.0	1.802	1.257	1.440	33.8	.120	5.06	3.55	9	
					8.1	95.5	91.5	2.165	1.440	1.528	41.9	.164	5.43	3.91	9	
21	31	2.35	Tubular	6(a)	29.5	111.0	90.5	2.059	1.200	1.372	29.5	0.086	2.92	2.92	9	
					12.2	96.0	90.5	2.173	1.372	1.483	41.7	.142	4.55	3.41	9	
22	69	2.35	Contour	6(b)	33.0	101.5	91.5	1.961	1.200	1.275	33.0	0.038	1.15	1.15	9	
					19.2	100.5	90.0	1.950	1.275	1.418	52.2	.109	3.72	2.09	9	
					12.4	97.0	90.5	1.984	1.418	1.517	64.6	.159	3.99	2.46	9	

^aAborted after 10.9 and 2.8 sec.



Figure 1. - Small storable-propellant rocket-engine test facility.

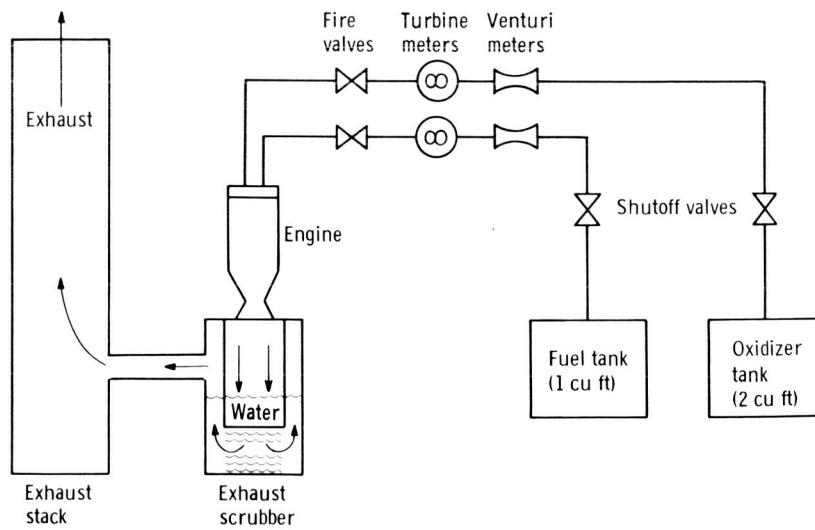
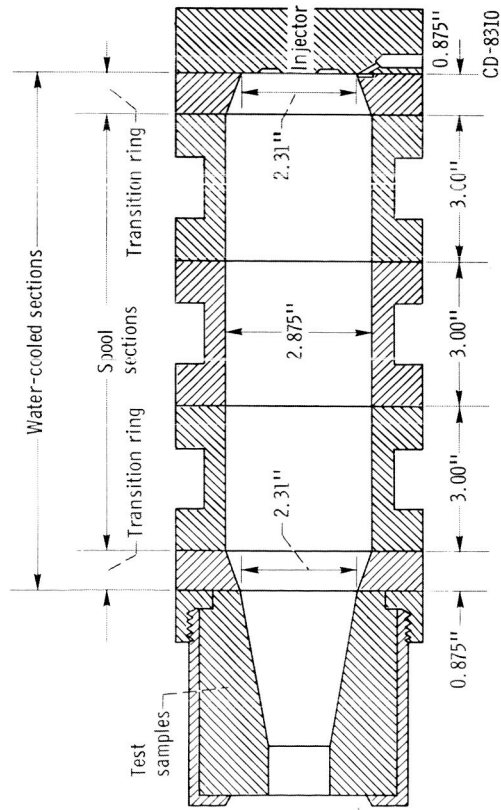


Figure 2. - Test installation.



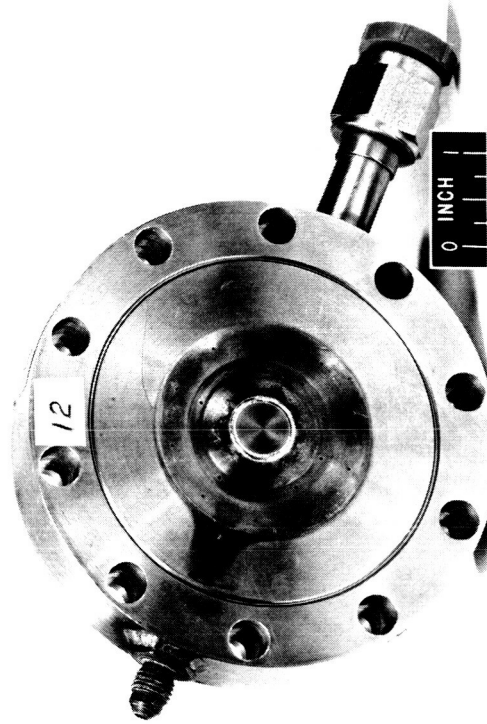
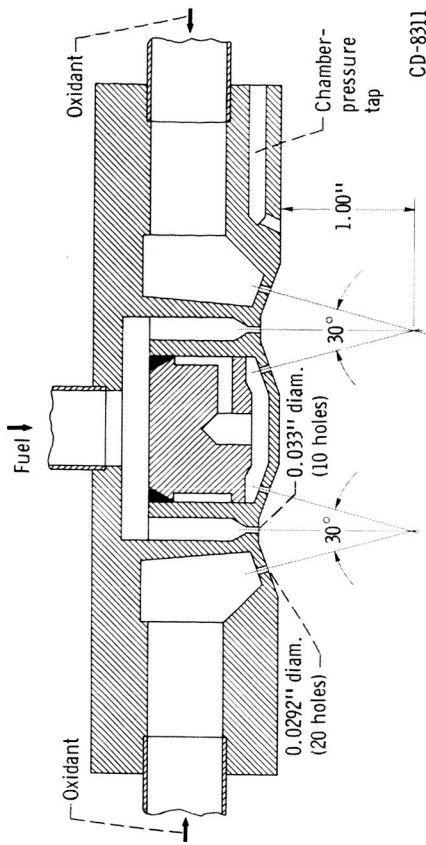
C-74287

(a) Disassembled.



(b) Assembled.

Figure 3. - Engine configuration.



C-70057

Figure 4. - Injector configuration.

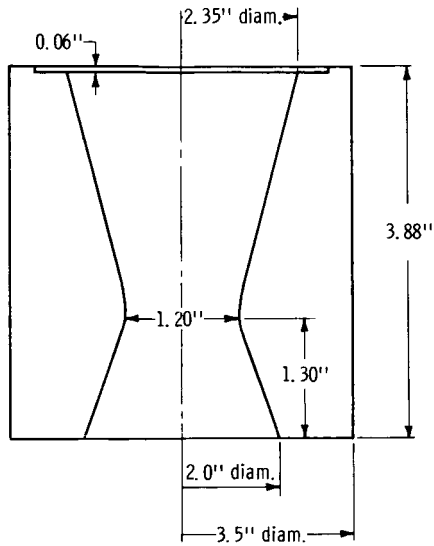


Figure 5. - Copper heat-sink nozzle.

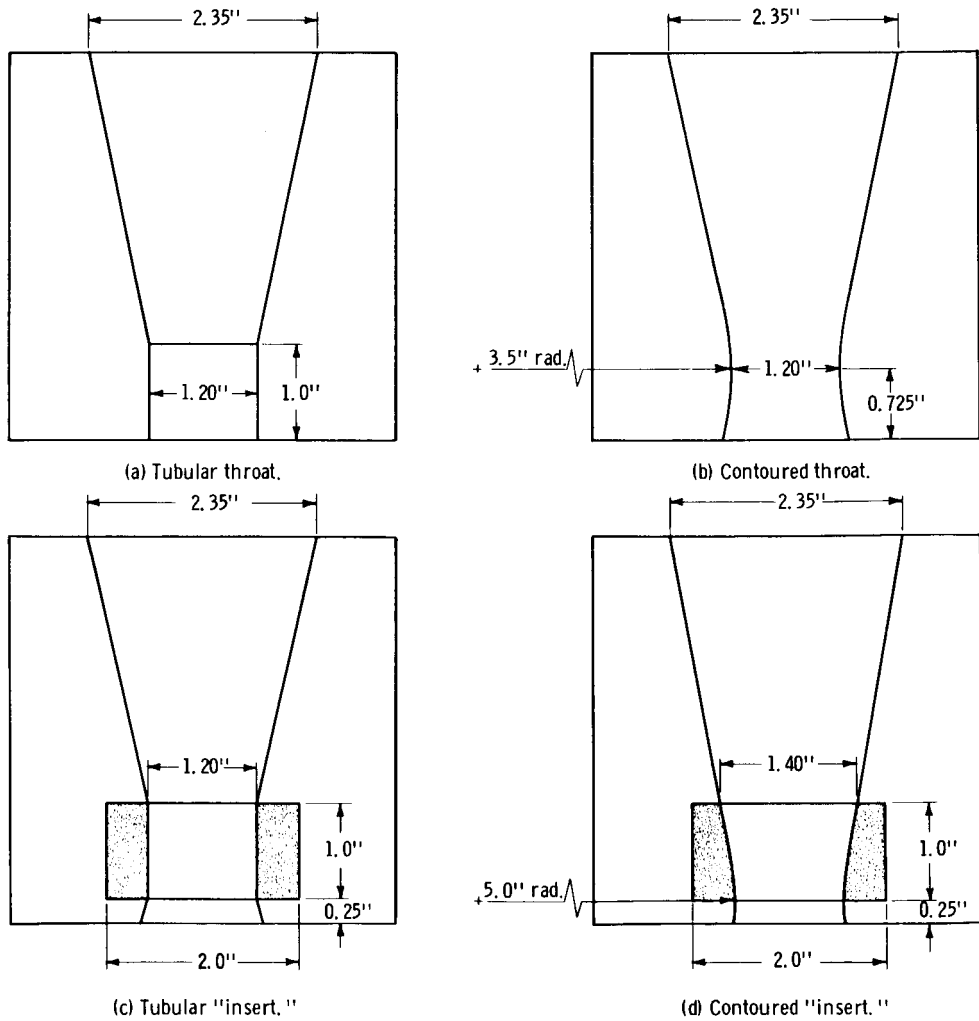
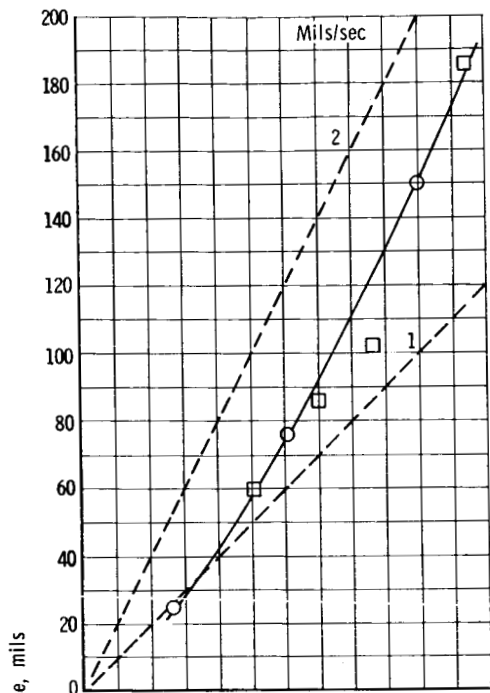
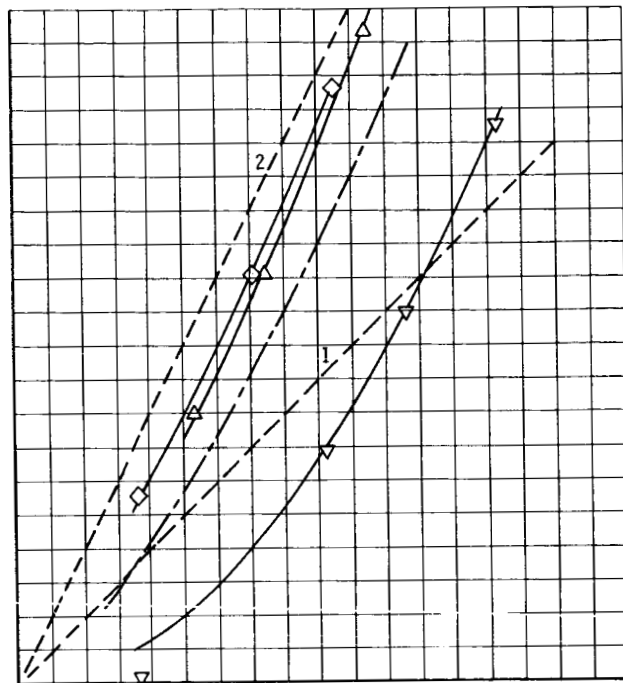


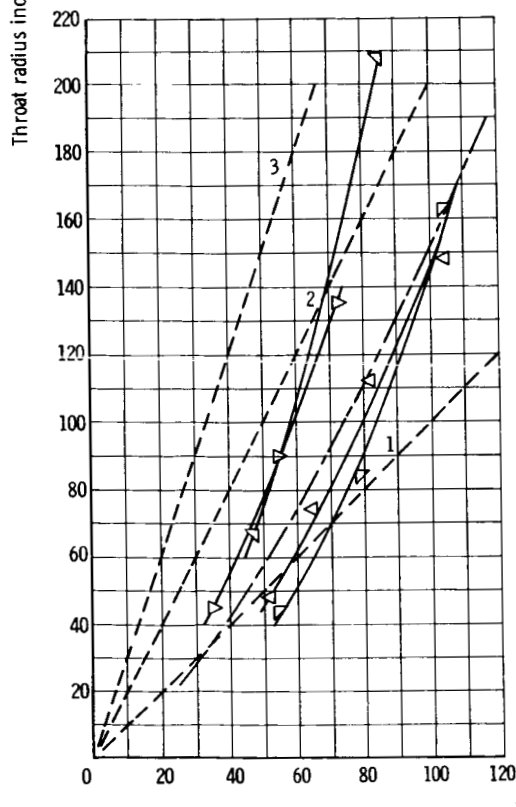
Figure 6. - Ablative-material nozzle configurations.



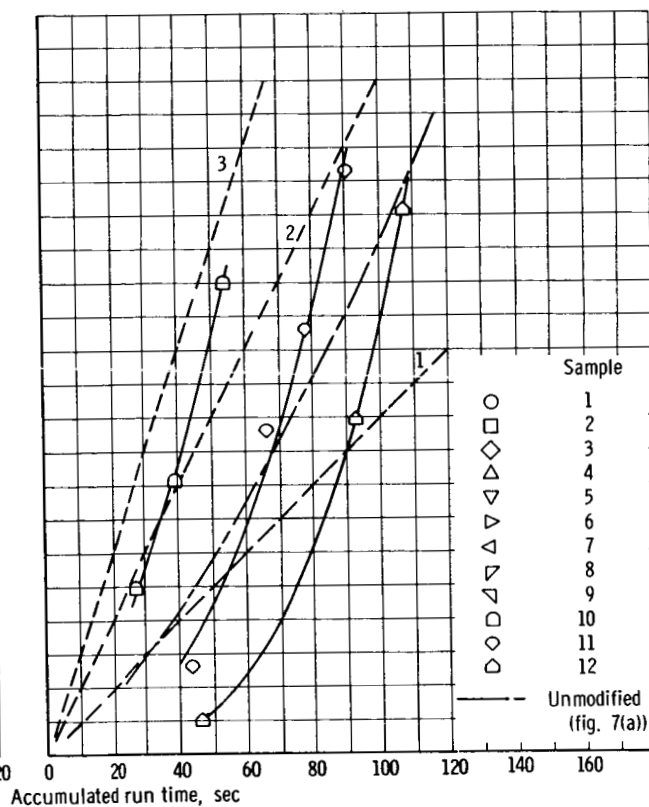
(a) Without modifications.



(b) Modified with silica.



(c) Modified with polyamide.



(d) With various modifications.

Figure 7. - Increase in throat dimension as function of accumulated run time for ablative materials with silica-cloth reinforcement and phenolic resin.

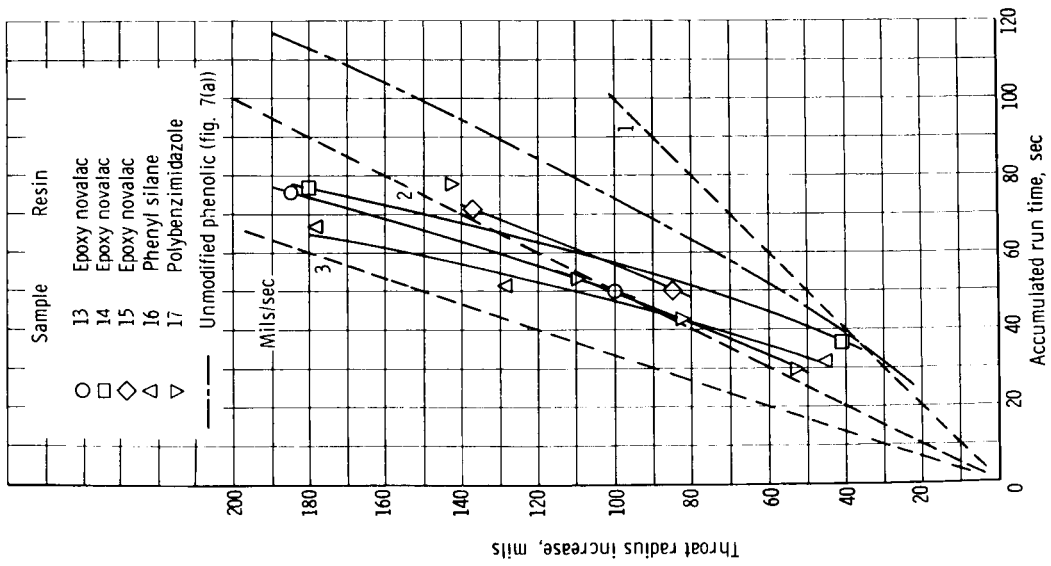


Figure 8. - Increase in throat dimension as function of accumulated run time for ablative materials with silica-cloth reinforcement and resins other than phenolic.

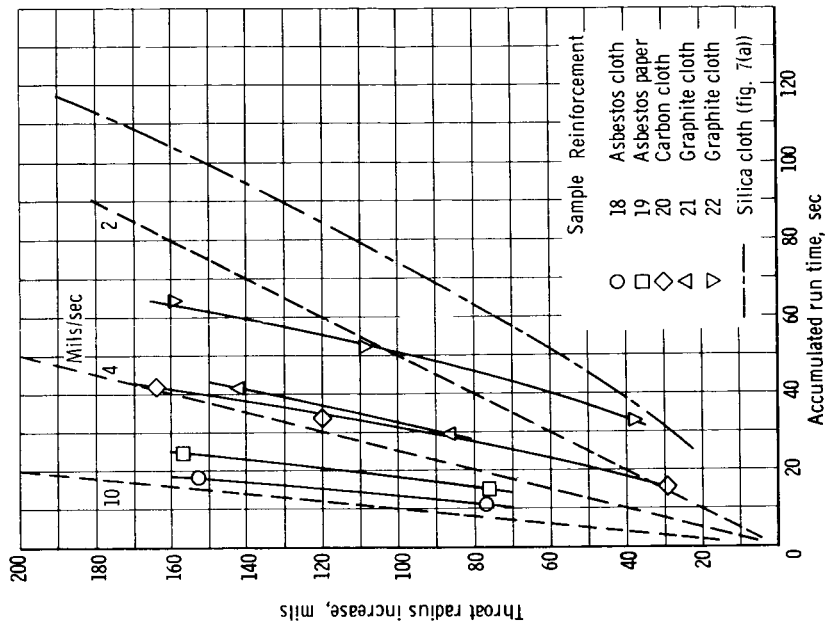


Figure 9. - Increase in throat dimension as function of accumulated run time for ablative materials with phenolic resin and reinforcements other than silica cloth.

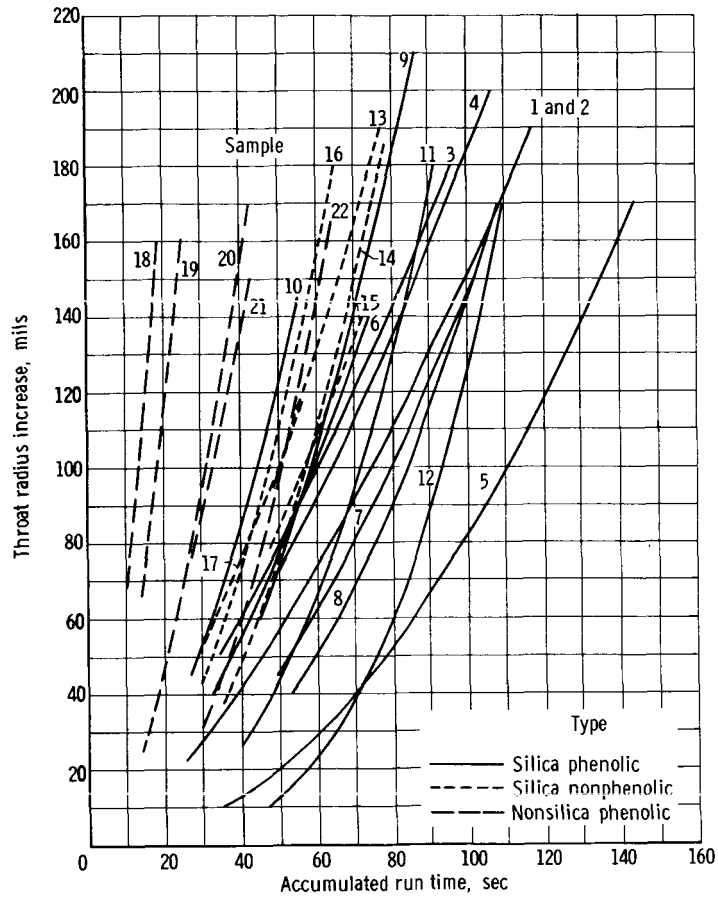
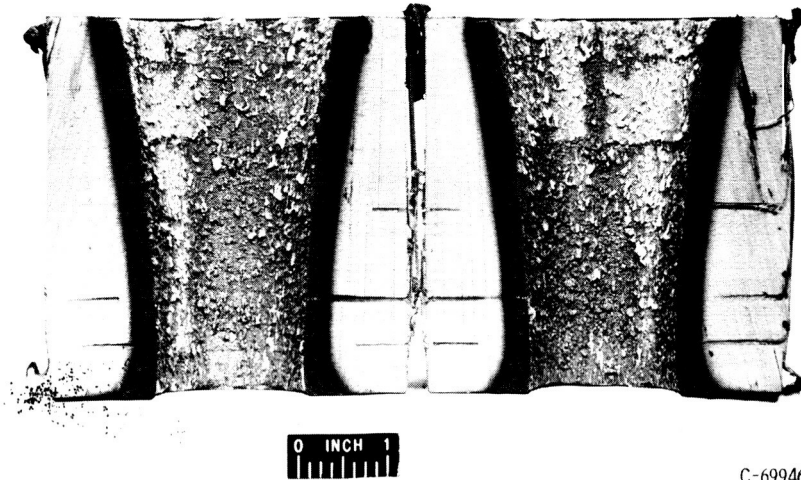
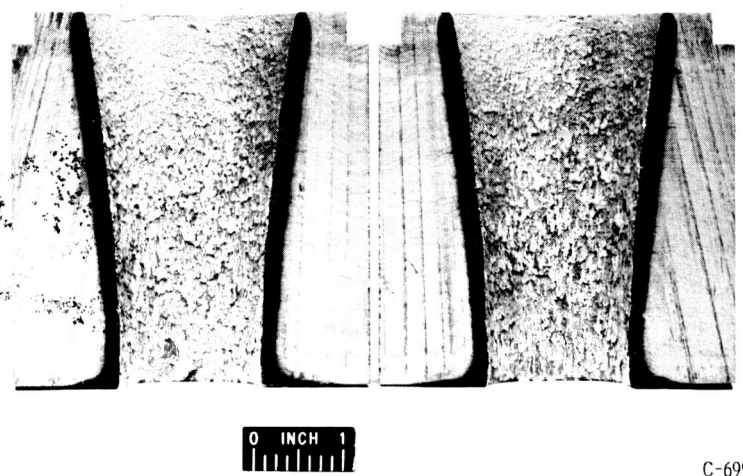


Figure 10. - Summary comparison of increase in throat dimension as function of accumulated run time.



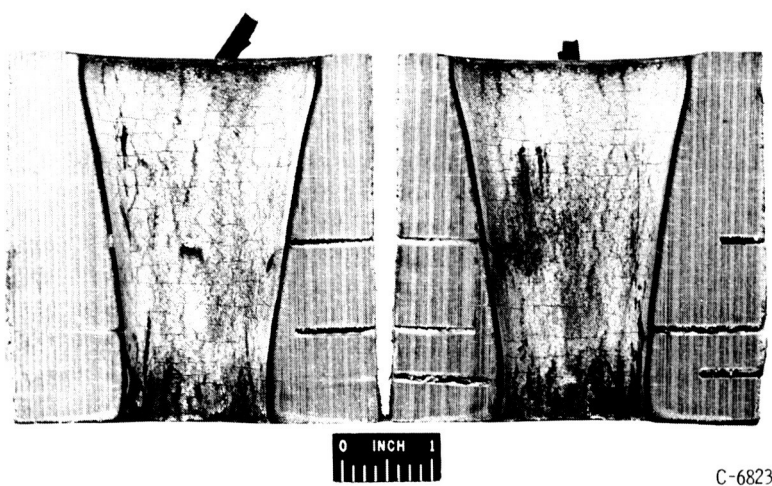
C-69946

(a) Sample 1 (silica-cloth reinforcement and phenolic resin (unmodified)).



C-69945

(b) Sample 10 (silica-cloth reinforcement and phenolic resin with inorganic additive).



C-68231

(c) Sample 19 (asbestos reinforcement and phenolic resin).

Figure 11. - Postfiring char formation.